

Chapter 2

Literature Review

2.1 Basic concepts of turbulent gas-particle flow

The turbulent gas-particle flows investigated in this thesis are all dilute. According to Loth (2000), the gas-particle flow is considered ‘dilute’ when the effects of particle-particle interactions are not significant. The effects include two separate mechanisms: particle-particle collisions and particle-particle dynamic interactions. The effect of particle-particle collisions can be neglected if the time-scale of particle-particle collisions is much longer than either the fluid dynamic particle relaxation time τ_p or the time-scale of turbulent particle-eddy interactions τ_{int} . The second criteria of dilute gas-particle flows is that particles do not influence each other with respect to fluid dynamic forces, i.e. such influence will only occur a small fraction of the time (Loth, 2000).

When the gas-particle flow is dilute, the influence of the particle phase on the gas phase may be negligible and this is referred as to ‘one-way coupling’. In other words, only the effects from gas phase to particle phase are taken into consideration. Elghobashi (1994) proposed a relationship between the related parameters of volume fraction and particle-turbulence interaction. He suggested that the particles will not influence the carrier phase when the particle phase volume fraction α_p is less than 10^{-6} . Here, α_p is defined as

$$\alpha_p = \frac{\dot{m}_p}{\rho_p} \quad (2.1)$$

where \dot{m}_p is the mass of particles in per unit volume of the mixture and ρ_p is the particle density. For volume fraction between 10^{-6} and 10^{-3} the effects from particles to carrier phase should be considered. It is so-called ‘two-way coupling’. For flow with volume fraction above 10^{-3} , the particle-particle interactions will occur as well as two-way coupling.

For gas-particle flows, the dimensionless number, Stokes number, presents an important criteria towards understanding the state of the particles whether they are in kinetic equilibrium with the surrounding gas. Stokes number is defined as the ratio between the particle relaxation time and fluid time scale, i.e.

$$St = \tau_p / \tau_f \quad (2.2)$$

where τ_p is the particle relaxation time that is the time for a particle, falling from rest in a quiescent fluid, to reach $(1-1/e)$ of its terminal velocity. τ_p is calculated as:

$$\tau_p = \frac{(2\rho_p + \rho_g)d_p^2}{36\mu_g} \quad (2.3)$$

where d_p is the particle diameter and ρ_p is the gas phase density. μ_g denotes the gas phase dynamic viscosity. As the particle densities are much larger than the gas phase density in this study, Equation (2.3) can be written as:

$$\tau_p = \frac{\rho_p d_p^2}{18\mu_g} \quad (2.4)$$

In Equation (2.2), a macroscopic Stokes number can be defined when the fluid time scale τ_f is determined from the characteristic length (L_s) and the characteristic velocity (V_s) of the system under investigation:

$$\tau_f = L_s / V_s \quad (2.5)$$

In contrast, one can obtain the microscopic Stokes number when the fluid time scale τ_f is calculated as a function of turbulence time scale, k_g / ε_g . For example, in the study of Tu and Fletcher (1995), τ_f is defined as:

$$\tau_f = 0.125 \frac{k_g}{\epsilon_g} \quad (2.6)$$

where k_g denotes the gas phase turbulent kinetic energy, and ϵ_g is the dissipation rate of turbulent kinetic energy. The Stokes number indicates how readily a particle follows the fluctuations of an eddy. For Stokes number much smaller than unity, the particle acts nearly as a passive tracer as it can quickly respond to the gas phase fluctuations. If Stokes number is much larger than unity, particle is mainly controlled by mean gas phase convection and gravity and does not respond to the gas phase fluctuations. For mediate Stokes number, particles that have higher density than gas can centrifuge out of eddy cores (Loth, 2000).

2.2 Numerical approaches for gas-particle flow

2.2.1 Eulerian-Eulerian model

The Eulerian-Eulerian model simulates the particle phases via fluid-like equations. One of its advantages is that it is easy to implement, solve and interpret along with the fluid phase equations (Shirolkar et al., 1996). As well, it can be handled efficiently through current state-of-the-art solvers resulting in a relatively less computational time of mean parameters for the particle flow. These advantages make the Eulerian-Eulerian model attractive and lately, there are possible considerations of extending the two-fluid model adopting the LES approach (Pandya et al., 2002) to circumvent the problems associated with current turbulence modelling.

Nevertheless, there are some inherent difficulties in the use of Eulerian-Eulerian model for gas-particle flows. The first difficulty arises in the modelling of the surface boundary conditions for the particle phase. The current Eulerian formulation is still deficient in correctly describing the aerodynamics drag force on the particle phase in the vicinity of a solid wall. The attempt of properly quantifying the incident and reflected particles during the process of particle-wall collision in a control volume at the boundary surface is still far from adequate resolution. More information regarding the particle behaviours is still

required to develop suitable models to better represent the particle-wall impaction process (Tu, 2000, Tu et al., 2004).

To overcome the problem of modelling particle-wall collision, Tu and Fletcher (1995) established a set of Eulerian formulation with generalised wall boundary conditions and developed a particle-wall collision model to better represent the particle-wall momentum transfer. Here, good agreement with the experimental data was achieved using this model to investigate the gas-particle flow in an in-line tube bank. Later, Tu (1997) employed this model with overlapped grids to simulate the gas-particle flow over a backward facing step and in a T-junction channel. The model also yielded encouraging results where good agreements between the predictions and experimental data were found.

Another problem with the Eulerian-Eulerian model is the justification of the continuum assumption as the particles equilibrate with neither local fluid nor each other when flowing through the flow field (Shirolkar et al., 1996). The Eulerian-Eulerian model describes the averaged local particle parameters instead of the individual particle trajectory. This introduces the problem of “crossing trajectories” (Slater et al., 2001), and the lost of the particle properties could be significant when considering the local reaction rate of a particle that is essential for reacting flow systems (Shirolkar et al., 1996).

Also, the problem of numerical diffusion exists when the finite difference scheme is used to discretize the partial differential equations in Eulerian-Eulerian model (Shirolkar et al., 1996). Fine mesh schemes that cost expensive CPU time are required to solve this problem. When the particle phase is poly-dispersed, i.e. the non-uniform particle diameter, each size group is treated as a separate continuous field. This requires more CPU time and storage (Shirolkar et al., 1996).

2.2.2 Eulerian-Lagrangian model

For the Eulerian-Lagrangian approach, the Eulerian equations of the gas phase are solved and the Lagrangian equations of particle motion are integrated by tracking individual particle through the flow field (Morsi et al. 2004). It provides detailed description of the particle motion including the effects of history and takes into consideration all the forces

acting on the particles (Zhang et al., 2002). Eulerian-Lagrangian model is typically much more robust when the following flow properties are of interest: particle reflection from surfaces; counter-flowing particles; significant poly-dispersion of size, velocity or temperature; and turbulent diffusion (Loth, 2000). In addition, non-physical numerical diffusion of Eulerian particle density in regions of high gradients can be eliminated by employing Eulerian-Lagrangian model (Loth, 2000).

Several models in the Lagrangian framework have been developed recently, such as the deterministic separated flow (DSF) model (Faeth, 1987), stochastic model, and particle cloud tracking model (Baxter and Smith, 1993). Among these models, DSF and Stochastic model have been widely used in predicting particle dispersion (Zhang et al., 2002), since they are easy to implement and able to take into consideration the complex particle phenomena (Crowe et al., 1998).

In DSF model, the influence of gas phase turbulence on the particle phase is neglected by using the time-averaged fluid velocity, u_i^g , at the particle location as the instantaneous fluid velocity to calculate the particle trajectory. This model is deterministic as once the average Eulerian fluid velocity is known, the particle trajectories can be directly computed (Shirolkar et al., 1996). The DSF model is easy to implement in CFD codes and does not require a large number of trajectories for a statistical solution (Zhang et al., 2002). Nevertheless, DSF has the inherent difficulty when the effect of gas phase turbulence on the particle dispersion is not negligible.

The main idea in the application of stochastic method is to introduce a large number of particles into the flow of interest and to generate a ‘synthetic’ turbulence with some known statistical properties, such as the mean and variance of the fluid fluctuating velocity (Mashayek and Pandya, 2003). Two kinds of stochastic models have been proposed: (i) random walk model; (ii) stochastic differential equations (SDE) model. The SDE model typically does not require the drift correction for non-homogeneous flows as its first-moment is identical to the Eulerian momentum equation (MacInnes and Bracco, 1992). Nevertheless, the SDE model requires the Reynolds-stress transport description of the turbulence, typically including modelling of triple-moments. It has not been tested extensively in particle-laden flows (Shirolka et al., 1996). Furthermore, it becomes

complicated for wall interactions as it requires Eulerian-type boundary conditions which cannot robustly handle wall reflection (Loth, 2000). Therefore, SDE model can not be generally recommended for engineering application yet (Shirolka et al., 1996).

First proposed by Taylor (1920) and implemented in the numerical simulation by Hotchkiss and Hirt (1972), the random walk model specifies the gas velocity as the sum of the time-averaged velocity and a random fluctuating velocity, or fluctuating velocity increment in some models, selected from a Gaussian distribution having zero mean and a variance related to the turbulent velocity scale coming from the turbulence model used in the Eulerian gas phase solution. Such Random walk model may be either continuous or discrete, according to the scheme for simulating the tendency of the current velocity fluctuation to change with time or position (Macinnes and Bracco, 1992).

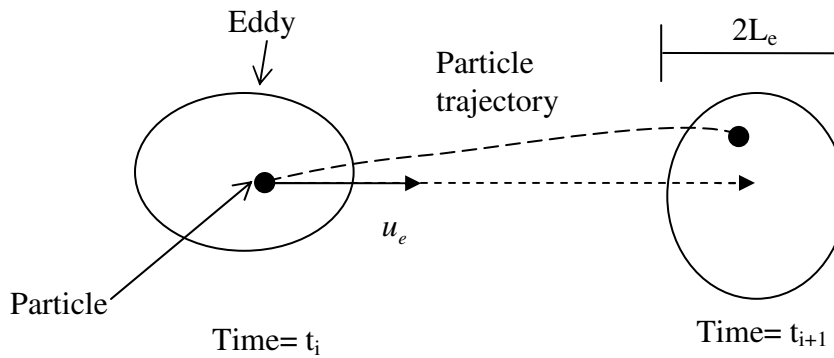


Figure 2.1 Eddy-particle interaction model.

With the discrete random walk (DRW) models, the turbulent dispersion of a particle is considered based on the concept of energy containing eddies. Here, the broad spectrum of turbulent eddies are simplified by local mean eddies which are characterized by a single eddy strength (base on turbulence intensity), the eddy lifetime τ_e , an eddy length scale L_e , and a time-averaged velocity (Loth, 2000). When the particles move through the turbulent gas flow field, they are assumed to interact with the local turbulent gas eddies, which are represented by an instantaneous gas velocity consisting of a time-averaged velocity and a fluctuating velocity (Chan et al., 2000). Therefore, these models are also referred to as eddy-interaction models (EIMs). Figure 2.1 illustrates the fundamental idea of the DRW or EIM model. At the beginning of an eddy-particle interaction ($t = t_i$), the particle, with velocity u_{p0} , is assumed to be located at the centre of an eddy with an instantaneous fluid

velocity u_e . The instantaneous eddy velocity, u_e , which is the sum of a mean part and a fluctuating part, remains constant during the interaction temporally and spatially within the eddy. After some time (for example, $t = t_{i+1}$), the eddy has moved to the new location with the instantaneous fluid velocity. The particle normally has another trajectory according to its own velocity. If either the eddy lifetime is over or the particle crosses the eddy (the distance between the particle and eddy centre is larger than the eddy length scale, L_e), a new interaction starts.

The gas phase fluctuation velocity is obtained by sampling a random number which satisfies a predefined probability density function, usually Gaussian distribution. It is discrete or ‘discontinuous’ as the random number is independent of each other from one eddy to another eddy (Gao, 2003). In DRW models, concerns are mainly focused on how to determine the eddy lifetime τ_e , eddy length scale L_e , and the interaction time between the particle and eddies τ_{int} . One early DRW model was found in the study of Gosman and Ioannides (1981). In their model, the gas phase turbulence was assumed to be isotropic. The fluctuating velocity components that prevail during the lifetime of the turbulent eddy are sampled by assuming that they obey a Gaussian probability distribution which has a zero mean and variance with value of $2k_g/3$. The eddy length scale is determined as following:

$$Le = \frac{C_\mu^{3/4} k_g^{2/3}}{\epsilon_g} \quad (2.7)$$

And the eddy lifetime is then calculate by:

$$\tau_e = \frac{Le}{|u'_g|} = \frac{C_\mu^{3/4} k_g^{2/3}}{\epsilon_g |u'_g|} \quad (2.8)$$

The eddy crossing time is computed by:

$$\tau_{cross} = -\tau_p \ln \left[1 - \left(\frac{Le}{\tau_p |\mathbf{u}_g - \mathbf{u}_p|} \right) \right] \quad (2.9)$$

where C_μ is a constant. $|\mathbf{u}_g - \mathbf{u}_p|$ is the magnitude of the relative velocity.

The eddy-particle interaction time is the smaller of the eddy lifetime or the eddy crossing time that accounts for the crossing trajectory effect, i.e.

$$\tau_{int} = \min(\tau_{cross}, \tau_e) \quad (2.10)$$

The above model and many of its variants have been used to simulate the gas-particle flows. Faeth and coworkers (Shuen et al., 1983; Shuen et al., 1985) employed this model to investigate the particle-laden jet and found the good agreement between the prediction and experimental data. Azevedo and Pereira (1990) utilized a variant of this model to simulate the both the free and confined particle-laden jet flows. In their model, the eddy lifetime is

calculated as $\tau_e = 0.3 \frac{k_g}{\epsilon_g}$ and the eddy crossing time is defined as

$$\tau_{cross} = \sqrt{\frac{2}{3} k_g \tau_e} / |\mathbf{u}_g - \mathbf{u}_p|.$$

The original DRW model of Gosman and Ioannides (1981) was capable of accounting for the crossing trajectories effect (CTE), which was first specified by Yudine (1959). The CTE means that a particle migrates from one eddy to another eddy, due to the turbulence of the original eddy, before the original eddy decays.

The original DRW model uses the constraint that eddy-particle interaction times can never exceed the corresponding interaction times for fluid particles (Graham, 1998). This leads to the prediction that heavy particles will be dispersed less rapidly, in the long-time limit, than fluid particles. Actually, it is contrary to the analytical and experimental results (Reeks, 1977; Squires and Eaton, 1991) which show that dispersivity can increase with particle inertia, a phenomenon called the inertia effect (Graham, 1998). Graham (1996)

proposed a modified DRW model that has two different time scales to overcome this problem. In this modified model, the finite-inertia particles can interact with eddies up to a maximum interaction time τ_{\max} that can be larger than the interaction time for fluid particles.

Also, the original DRW model of Gosman and Ioannides (1981) does not take into consideration of directional anisotropy in anisotropic flows. Some modifications have been proposed to remedy this problem. Wang and James (1999) introduced damping functions into the original DRW model, within the framework of k - ε model, to handle the anisotropy in near wall regions. Chen and Pereira (1991) used the Reynolds-Stress model (RSM) for the fluid phase. The normal stresses $\sqrt{u'_i u'_i}$ are used instead of $\sqrt{2k_g/3}$ to calculate the fluctuating velocity.

Another shortcoming of DRW model is that it may give non-physical results in strongly inhomogeneous diffusion-dominated flows, where small particles (such as scalar particles) should become uniformly distributed. Instead, the DRW will show a tendency for such particles to concentrate in low-turbulence regions of the flow (MacInnes and Bracco, 1992). Underwood (1993) found that it can lead to an order of magnitude error in particle deposition rates for turbulent channel flow. Bocksell and Loth (1998) suggested correcting this artificial drift by shifting the random DRW velocity by using a summation to integrate overall previous timestep:

$$u'_{i,drift} = \sum \Delta t d(u'_{i,drift}) / dt \quad (2.11)$$

This correction gave superior results with respect to scalar conservation (Loth, 2000).

Some continuous random walk (CRW) models have been developed to avoid the discontinuity (Berlemont et al., 1990; Zhou and Leschziner, 1991). Including the turbulence correlations, CRW models improve the representation of the turbulence as the velocity fluctuations are continuous in time.

However, the DRW models have been widely used (Faeth, 1987, Crowe et al., 1998) due to its simplicity and computational efficiency, and have shown remarkable performance in complex flows (Loth, 2000). This study employs the DRW model that is available in the CFD package FLUENT.

2.3 Turbulence models for gas phase

Many, if not most, flows of engineering significance are turbulent in nature. The turbulent flow regime is, therefore, not just of theoretical interest among the academics. Engineers that are interested in fluid flows need access to viable tools capable of representing the effects of turbulence.

There are three techniques currently available to numerically solve the turbulence flow. They are: direct numerical simulation (DNS), Reynolds averaged Navier-Stokes (RANS) and LES.

DNS directly solves the Navier-Stokes equations of the gas phase. It provides the most accurate solutions as all of the motions contained in the flow are resolved. DNS of gas-particle flows have been conducted in three configurations (Mashayek and Pandya, 2003): (i) isotropic homogeneous flow (Boivin et al., 1998); (ii) anisotropic homogeneous flow (Ahmed and Elgohbashi, 2001); (iii) inhomogeneous flow (Pedinotti et al., 1992). However, extremely fine meshes and small time steps are required by DNS to solve the smallest eddies. The total number of grid points necessary to solve a turbulent flow by DNS is proportional to Re_L^3 in three dimensions (Tennekes and Lumley, 1976). For example, the smallest eddies in an indoor airflow are typically within the size of 0.1 to 1 mm. In order to solve these small eddies by DNS, the total grid number for a three-dimensional indoor airflow is around 10^{11} to 10^{12} (Spengler et al., 2001). That is impossibly expensive in view of the computational standing for engineering flows. Thus, DNS is only useful as a basic research tool for flows with very low Reynolds number and simple geometry (Ferziger and Peric, 2002).

The descriptions of large eddy motions are of main interest in complex flows as larger eddies generally transport most of the momentum or thermal energy. LES has been developed to take advantage of this fact. In LES, large-scale quantities of flow from the filtered Navier-Stokes equations are solved directly and the small eddies are modeled by the subgrid-scale (SGS) model. Therefore, it requires much less computing expense than DNS.

Many SGS models have been developed such as the Smagorinsky and related models (Smagorinsky, 1963) and dynamic models (Pierre, 1998). Amongst these SGS models, a SGS model based on the RNG theory has been formulated by Yakhot et al. (1989). This RNG-based LES model is able to provide the description of the low-Reynolds-number and near wall flows that are always encountered in indoor air flows. Karniadakis et al. (1990) employed this RNG-based LES model to simulate flows over a backward facing step geometry at different Reynolds numbers ($Re = 2222, 4444, 8888$, respectively). They validated the simulation results against experimental data and found that the discrepancy was less than 10%.

In the RANS approach for modeling turbulence, an approximation is introduced that all the flow unsteadiness is averaged out and the nonlinearity of the Navier-Stokes equations gives rise to terms that must be modeled. RANS model is quick, simple and possesses good numerical stability. When the model is properly applied, it provides reasonable results (Chen, 1997). The two-equation $k-\varepsilon$ model is the most popular and used RANS turbulence model for the numerical simulation of gas-particle flows. It is easy to program and modify whilst giving reasonable results in many applications (Chen, 1997).

2.4 Particle-wall collision models

It is necessary to apply detailed physical models for the particle-wall interaction in numerical simulations of confined, wall-bounded gas-particle flows, since the particle wall collision is one of the governing phenomenon in such flows (Sommerfeld and Huber, 1999). When reaching a wall surface, a particle either deposits on or rebounds from the wall. If the particle incident velocity is below a certain value, called the capture (or critical) velocity, it may remain attached to the wall (Brach and Dunn, 1998). If the particle

incident velocity is above the capture velocity, it may bounce with a momentum loss. Several physical parameters govern the particle-wall collision process. Among these parameters are the particle incident velocity, initial angular velocity, incident angle, diameter and shape of the particle as well as its material properties. Other parameters such as the surface characteristics and roughness can also contribute to significantly influence the particle impacting on and rebounding away from the wall surface (Li et al., 2000; Sommerfeld, 1992). Despite the many experimental and computational investigations conducted by Matsumoto et al. (1970), Dahneke (1975), Grand and Tabakoff (1975), Tsuji et al. (1987), Sommerfeld (1992), Brach and Dunn (1992, 1998), Sommerfeld and Huber (1999) and many others, the success in properly modeling the particle-wall collision process remains elusive due to its complex nature.

For dilute gas-particle flows, three basic categories of particle-wall collision models are currently used in Lagrangian particle-tracking models:

- In the first kind of model, the normal and tangential coefficients of restitution are taken as constants, i.e. $e_n = -\frac{v_n^p}{u_n^p} = \text{constant 1}$, $e_t = \frac{v_t^p}{u_t^p} = \text{constant 2}$ (see Figure 2.2). The subscript n and t represent the normal and tangential direction, respectively. And u_p and v_p refers to the particle incident and rebounding velocity components, respectively.
- The second kind of collision model treats the values of normal and tangential coefficients of restitution as the correlations of particle incident angles, θ , $e_n = f_n(\theta)$ and $e_t = f_t(\theta)$.
- The third kind of collision model comprises a set of equations that are based on the particle impulse and moment equations (Sommerfeld, 1992). In this model, the normal restitution coefficient, the static friction coefficient and the dynamic friction coefficient are obtained from experiments.

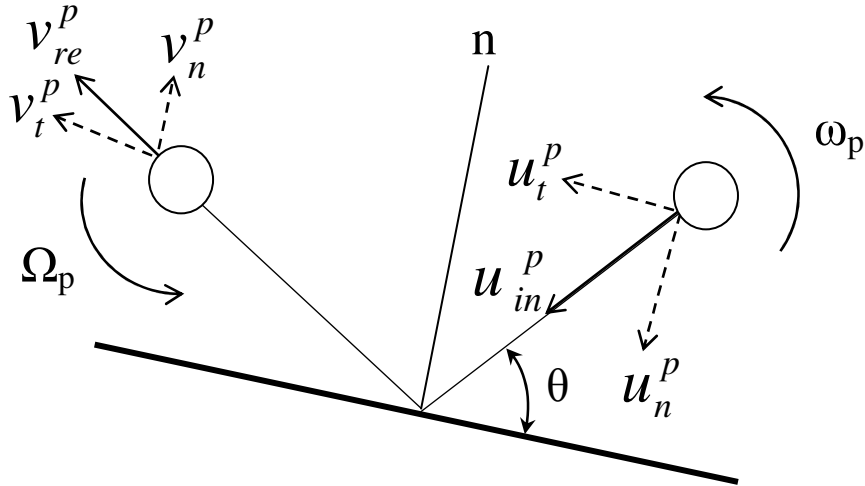


Figure 2.2 Particle-wall collision configuration

The first kind of collision model is based on the laws of mechanics and the two suppositions. Here, the contact area between a particle and a wall surface is treated as a point. It assumes that the normal particle restitution coefficient is a constant that is independent on the particle incident velocity, particle incident angle and the surface materials (Tsirkunov and Panfilov, 1998). And this kind of model sometimes assumes that there is no tangential force acting from a wall on a particle. When the perfectly elastic impacts are assumed, the normal and tangential particle restitution coefficients are set to unity (Tsirkunov and Panfilov, 1998). This kind of model is easy to understand and to be implemented into CFD code. Further, no extensive experiments are required to obtain the restitution coefficients. It may be used for the gas-particle flows when the particle-wall bouncing is not important for particle phase simulation. One example of is the gas-particle flow with relatively small particles, since the small particles promptly follow carrier fluid after a collision (Sommerfeld, 1992).

The second kind of model is purely empirical, since all parameters in the correlations are determined through experiments. The rebound dynamics of particles are described in a statistical sense. Grant and Tabakoff (1975) explained this as the results of eroded wall surface and irregular particle surface. The target wall surface will become pitted with craters after a given incubation period. Further after a slightly longer time, a regular ripple pattern may form on the eroded surface. As a result, the local incident angle between the particle and eroded surface may deviate considerably from the geometric average (Grant

and Tabakoff, 1975). The irregular particle shape may also considerably influence the particle rebounding performance. However, this is not within the focus of this study as all particles herein are assumed to be sphere.

Tabakoff and co-workers conducted a series of experiments to obtain the parameters in the correlations for several particle-wall collision cases. Grand and Tabakoff (1975) measured the restitution and erosion parameters using high-speed photography. The mean normal and tangential restitution coefficients of 200 μm quartz particles impacting on 2024 aluminum surface were fitted by least squares polynomial curves. The equations are as following:

$$\begin{aligned} e_n &= -\frac{v_n^p}{u_n^p} = 0.993 - 1.76\theta + 1.56\theta^2 - 0.49\theta^3 \\ e_t &= \frac{v_t^p}{u_t^p} = 0.988 - 1.66\theta + 2.11\theta^2 - 0.67\theta^3 \end{aligned} \quad (2.12)$$

where θ is the particle incident angle (degrees).

The equations for the standard deviation of the normal and tangential restitution coefficients were also calculated to handle the effect of incident angle on the statistical behavior. Later, Tabakoff et al. (1987) employed the laser Doppler velocimetry (LDV) to investigate the dynamic impact characteristics of erosive fly ash particles impacting on 2024 aluminum and 6A1-4V titanium surface. As well, mean restitution coefficients were analyzed and represented by least squares polynomial curve fits. Eroglu and Tabakoff (1991) carried out three-dimensional LDV measurements of particle-wall collision and found that three-dimensional rebound characteristics did not differ from the two-dimensional rebound characteristics. Tabakoff et al. (1996) measured the restitution characteristics of 150 μm silica sand particles colliding on the different materials including 2024 aluminum, 6A1-4V titanium, AM 355 steel and RENE 41. A similar trend in rebound characteristics was showed for all four materials.

Though the second kind of collision model is not universally applicable (Sommerfeld, 1992), it has been widely used to numerically investigate the gas-particle flows and surface erosion in various applications. Jun and Tabakoff (1994) simulated the dilute gas-particle

flow over tube banks using the parameters obtained in Grand and Tabakoff (1975). Employing the same parameters, Jin et al. (2001) studied the dilute gas-particle flow over staggered tube banks. Fan et al. (2002) investigated the performance of ribbed bend protection, a new method to protect duct bends against erosion, in gas-particle flows via the same model.

The third kind of collision model is based on the momentum equations and Coulombs law of friction. For a particle-wall collision procedure, two types of collision are distinguished: a collision with and without sliding (Mastumoto and Saito, 1970; Sommerfeld, 1992). At the end of contact with a wall, a particle is rolling when the following conditioned is satisfied:

$$\left| u_t^p - \frac{d_p}{2} \omega_p \right| < \frac{7}{2} \mu_0 (1 + e_n) u_n^p \quad (2.13)$$

where ω_p is the particle initial angular velocity. μ_0 is the static friction coefficient.

Under conditions of rolling collision, the rebound velocity components are as following

$$\begin{aligned} v_n^p &= -e_n u_n^p \\ v_t^p &= \frac{1}{7} (5u_t^p + d_p \omega_p) \\ \Omega_p &= 2 \frac{v_t^p}{d_p} \end{aligned} \quad (2.14)$$

If the particle is not rolling in the collision, it must be sliding and the rebound velocity components are defined as:

$$v_n^p = -e_n u_n^p$$

$$v_t^p = u_t^p - \mu_d (1 + e_n) \epsilon_0 u_n^p$$

$$\Omega_p = \omega_p + 5\mu_d (1 + e_n) \epsilon_0 \frac{u_n^p}{d_p} \quad (2.15)$$

Here, μ_d is the dynamic friction coefficient. ϵ_0 is the direction of the relative velocity between particle surface and wall obtained by:

$$\epsilon_0 = \text{sign} \left(u_t^p - \frac{d_p}{2} \omega_p \right) \quad (2.16)$$

The empirical values required in the above equations are the normal restitution coefficient, e_n , the static friction coefficient, μ_0 . The static friction coefficient and the dynamic friction coefficient are generally known for certain material combinations. However, depending on the properties of wall surfaces, some scatter may be possible (Sommerfeld, 1992).

Beside the above models, an algebraic particle-wall collision model has been developed by Brach and Dunn (1992, 1998). Based on Newton's laws in the form of impulse and momentum (Brach et al., 2000), this algebraic collision model has the ability to deal with oblique collision and calculate the particle angular velocities (Brach and Dunn, 1998). Another distinguished feature of this model is that it can account for the particle deposition on the surfaces by introducing a critical or capture velocity. When the impact velocity is lower than the critical velocity, the particle is assumed to deposit on the surface.

For particles with diameters in the range of $1 \mu\text{m} \sim 100 \mu\text{m}$ and relatively high incident velocity, the particle rebound velocity follows the same trend, i.e. the restitution coefficient is almost constant when the particle incident velocity varies. Nonetheless, when the incident velocities become relatively low (below $\sim 10 \text{ m/s}$), the rebound velocities decrease remarkably. In other words, the normal restitution coefficients decline dramatically when the incident velocities reduce (Brach and Dunn, 1992). Thus, the fluency from the incident velocities onto the coefficients of restitution is not negligible. This algebraic particle-wall collision model has been developed to account for this phenomenon by formulating the

overall restitution coefficient as a function of the incident velocity. The details of this model will be given in Chapter 3.3.

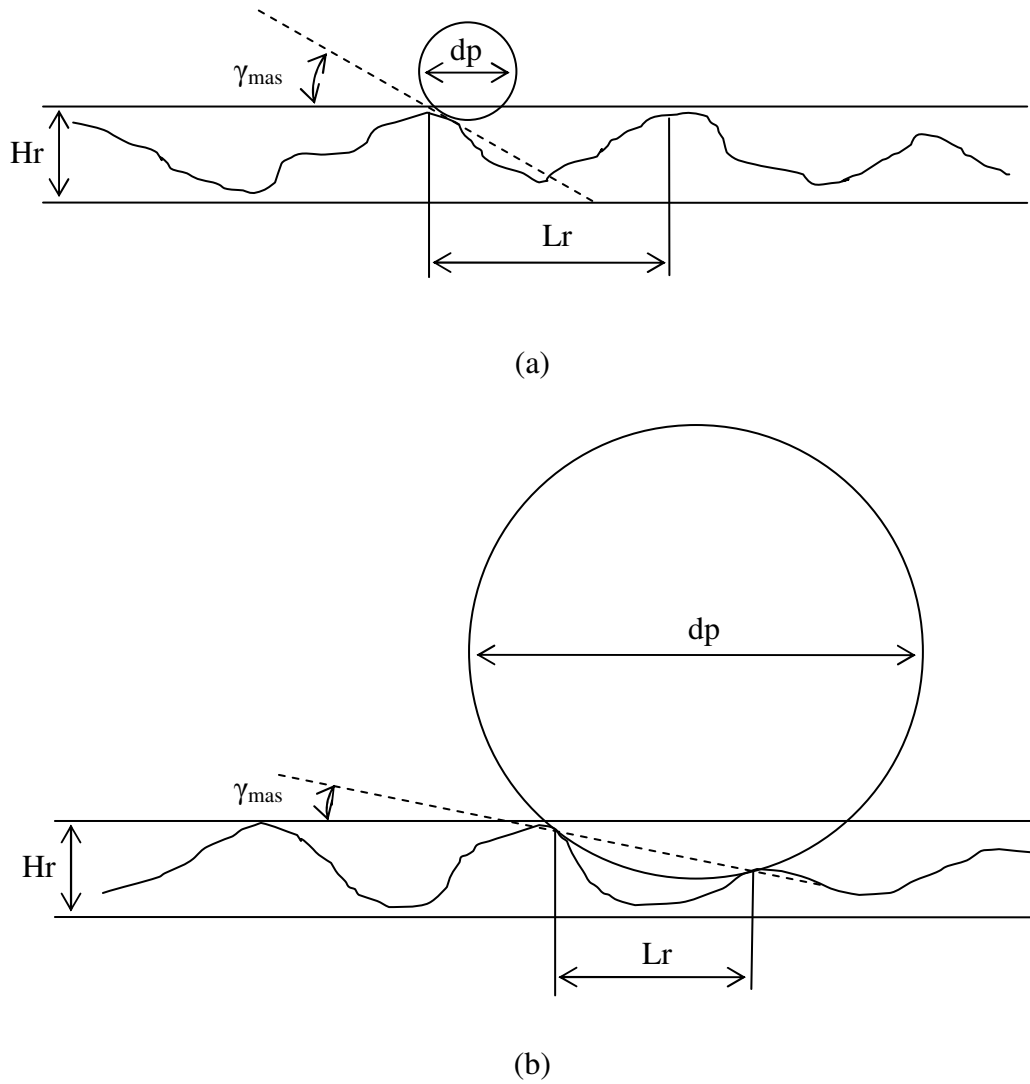


Figure 2.3 Particle-wall collision with wall roughness: (a) particle diameter larger than cycle of roughness and (b) particle diameter less than cycle of roughness.

The particle-wall collision model should also consider the wall roughness and the resulting stochastic nature of the process, since experimental investigations (Grand and Tabakoff, 1975; Govan et al., 1989) have found that the particle restitution coefficient is subject to some scatter due to wall roughness and non-spherical particles (Sommerfeld, 1992). Several models had been proposed to account for the effect of ‘wall roughness’ (Matsumoto and Saito, 1970; Tsuji et al., 1987; Sommerfeld, 1992). One notable finding whilst employing a traditional particle-wall collision model without incorporating wall-roughness was that particles eventually deposited at the bottom of the channel, which had been demonstrated in the numerical study of gas-particle flow in the horizontal channel by

Tsuji et al. (1987). That appeared to be inconsistent with experimental observation since it clearly showed that the particles continued to be suspended in the free-stream flow.

The wall roughness can be characterized by two important parameters, the mean roughness depth (H_r) and the mean cycle of roughness (L_r), that are illustrated in Figure 2.3 (Sommerfeld, 1992). When the diameter of a small particle is less than the cycle of roughness ($d_p < L_r$), the maximum change of collision angle due to the roughness can be calculated as:

$$\gamma_{\max} = \arctan \frac{2H_r}{L_r} \quad (2.17)$$

When the diameter of the particle is larger than the cycle of roughness, the maximum roughness angle is reduced. For example, if assuming that the minimum roughness height is about $H/2$, the maximum roughness angle is $\gamma_{\max} = \arctan \frac{H_r}{2L_r}$ (Sommerfeld, 1992).

Matsumoto and Saito (1970) first took into account the effect of wall roughness in numerical simulation of gas-particle flows. In their paper, the irregular collision caused by the roughness was modeled as a sine function. Tsuji et al. (1985) used a ‘virtual wall’ model to simulate the gas-particle flow in a pipe. When the particle incident angle is less than a certain value, the plane wall was replaced by the virtual wall, (see Figure 2.4) i.e. the collision angle was increased by a value of γ :

$$\gamma = \begin{cases} 0 & (\theta > \beta) \\ -\delta(\theta - \theta') & (\theta \leq \beta) \end{cases} \quad (2.18)$$

with

$$\begin{aligned} \delta &= \frac{2.3}{Fr} - \frac{91}{Fr^2} + \frac{1231}{Fr^3} \\ \beta &= 7^\circ \\ Fr &= \frac{u_g}{\sqrt{gh}} \end{aligned} \quad (2.19)$$

where Fr is the Froude number, h is the pipe height and g is the gravitational constant. Later, Tsuji et al. (1987) treated the value of δ as a randomly distributed coefficient:

$$\delta = 5R^4 \left(\frac{2.3}{Fr} - \frac{91}{Fr^2} + \frac{1231}{Fr^3} \right) \quad (2.20)$$

where R is a random number in the range $[0,1]$. One major limitation of this roughness model is that it does not take into consideration of roughness effects when the collision angle is larger than 7° (Sommerfeld, 1992).

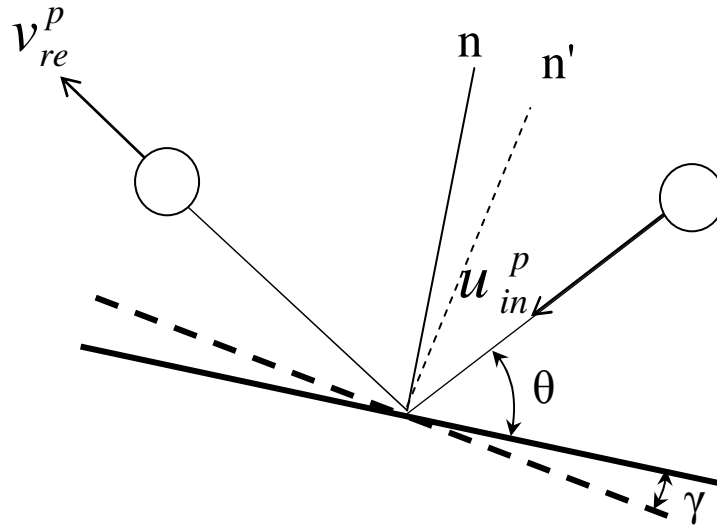


Figure 2.4 Virtual wall model for particle-wall collision.